# OPTIMIZATION OF THE PART-LOAD OPERATION STRATEGY OF SCO2 POWER PLANTS

Dario Alfani[1], Marco Astolfi[1]*, Marco Binotti[1], Ennio Macchi[1], Paolo Silva[1]

[1]Politecnico di Milano, Energy Department,
Milano, Italy
*marco.astolfi@polimi.it

## ABSTRACT

Supercritical $CO_2$ cycles for power generation are gaining a large interest from industry, institutions and academia as demonstrated by the large amount of investments, founded projects and research papers. This attention is motivated by the potential of $sCO_2$ technology of replacing conventional steam plants in a number of applications and likely to play a relevant role in the future energy scenario. The H2020 $sCO_2$-Flex project is studying the application of $sCO_2$ cycles in coal-fired power plants in order to enhance their flexibility and ease the integration with non-dispatchable renewable energy sources such as wind and solar. The $sCO_2$-Flex project has also the aim of investigating the replicability of the concept with other heat sources such as CSP, biomass and WHR. Main advantages of $sCO_2$ power plants with respect to USC technology are: (i) potential higher efficiency, (ii) compactness of the turbomachinery, (iii) no need of water treatment, deaerator, vacuum pump, etc., (iv) fast transients and (v) high performance at part-load. This study focuses on the last topic with the aim of investigating different part-load operation strategy for a waste heat recovery power plant based on a $sCO_2$ cycle exploiting a stream of 50 kg/s of flue gases at 550°C. The selected $sCO_2$ cycle is a recuperative recompressed cycle with high temperature recuperator bypass, whose maximum/minimum pressure and maximum temperature are optimized in design condition obtaining an overall recovery efficiency of 22.65%. Different operating strategies at part load are investigated considering the combinations of component features such as rotational speed and variable geometry at the inlet of turbomachinery, fan speed on the heat rejection unit, variation of the fluid inventory. The best operating strategy energy-wise is finally proposed, providing a numerical estimation of the off-design overall plant performance, highlighting the impact on the compressor operating points and on the fluid inventory variation within the cycle.

## 1. INTRODUCTION

The development of efficient power systems able to exploit a wide range of low-medium temperature heat sources is a topic of large interest for waste heat recovery (WHR) applications in many industrial fields. Currently, Organic Rankine Cycles is the most reliable solution for the exploitation of these energy sources since the alternative represented by steam cycles is characterized by an inefficient conversion efficiency for small available thermal powers.

However, the adoption of organic fluids involves several safety and environmental issues, either related to fluid flammability or to their high Global Warming Potential (GWP), which can lead to relevant complications and additional costs (Macchi and Astolfi 2016). To overcome these limitations supercritical $CO_2$ ($sCO_2$) cycles may represent an interesting option. In recent years $sCO_2$ cycles have been proposed for the exploitation of several energy sources such as coal (Mecheri and Le Moullec 2016), solar (Binotti et al. 2017) and WHR (Astolfi et al. 2018). The H2020 $sCO_2$-Flex project is studying the application of $sCO_2$ cycles in coal fired power plants in order to enhance their flexibility and ease the integration with non-dispatchable renewable energy sources. $sCO_2$-Flex will also evaluate the replicability of the concept with other heat sources such as CSP, biomass and WHR. The main advantages of $CO_2$ cycles are represented by (i) the high efficiency attainable with a compression process close to the working fluid critical point, (ii) the use of an environmentally

friendly, widely available, safe and thermally stable working fluid, (iii) the compactness and the limited number of components that may lead to a high system flexibility.
This study focuses on the part-load performance and control strategies for a $sCO_2$ cycle used as a power cycle to exploit a heat source constituted by a flue gas stream from a waste heat recovery process. Differently from Joule-Brayton closed cycles using ideal gases (He, $N_2$), in $sCO_2$ power plants the main compressor is generally designed to operate very close to the fluid critical point in a region characterized by marked real gas effects. For these plants, cycle depressurization at partial load may involve a significant variation of fluid properties along compression with an efficiency penalization that may jeopardize also the overall plant performance. The optimization of the part-load operation of $sCO_2$ power plants is scarcely studied in literature and the main unknowns regard the design and the operation of turbomachinery. In this work, different operating strategies are investigated for an optimized recuperative recompressed cycle configuration considering the combinations of component features: (i) turbine and compressor (fixed/variable velocity, with or without variable geometry), (ii) heat rejection unit (fixed/variable fan speed), (iii) fluid inventory (variable/fixed).
The best operating strategy, in terms of system efficiency, is proposed providing a numerical estimation of the part-load performance attainable with a WHR $sCO_2$ power cycle and highlighting suggested design criteria for the turbomachinery.

## 2. NUMERICAL CODE DESCRIPTION

In order to tackle the goal of this paper a dedicated numerical tool has been developed in MATLAB for the optimization of the system design and the evaluation of part-load operation. $CO_2$ thermodynamic properties are computed through the REFPROP 9.1 database (Lemmon et al. 2013) leading to an accurate evaluation of real gas effects close to the critical point of the working fluid.
With the developed numerical code several cycle configurations (more than 50 cycle schemes are proposed in literature (Crespi et al. 2017)) can be easily implemented, optimized and simulated over a large range of off-design conditions. A recompressed cycle with High Temperature Recuperator (HTR) bypass is considered in this work as one of the most promising cycle configurations for WHR application, although further analyses will include other cycle architectures and will provide a broader comparison among them. In all the recompressed cycles, a fraction of the main flow enters in the Heat Rejection Unit (HRU) where it is cooled down to the cycle minimum temperature, it is then pressurized by the main compressor and heated up in the Low Temperature Recuperator (LTR), while another fraction is split just before the HRU and it is compressed to the cycle maximum pressure by a secondary compressor. The two flows are eventually mixed at LTR cold side outlet. The recompression allows enhancing the efficiency of the cycle by balancing the heat capacities of the hot and cold streams of the LTR, limiting the temperature differences in the heat exchanger and the irreversibilities related to the heat transfer process. The simple recompressed cycle configuration is widely proposed in literature for solar tower applications (Polimeni et al. 2018; Ho et al. 2016; Binotti et al. 2017) mainly because of the high thermodynamic efficiency but in case of WHR application the $CO_2$ high temperature at the end of the internal recuperative process may limit the heat recovery from the heat source, reducing the heat input and eventually the power production. The introduction of the HTR bypass allows mitigating this issue by increasing the heat recovery factor and potentially leading to higher system performances. Plant scheme of the selected cycle configuration is reported in Figure 1.

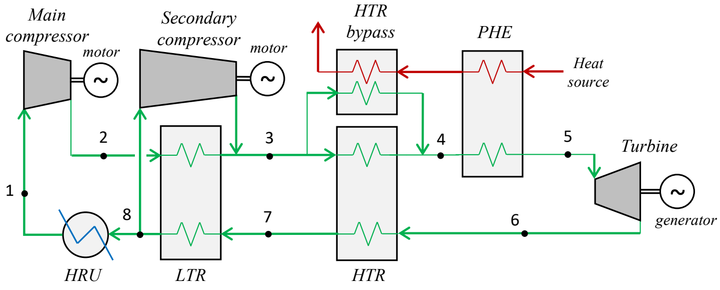


**Figure 1**: Schematic of the $sCO_2$ recuperative recompressed cycle with HTR bypass

### 2.1 Design optimization

The optimization of the system design is carried out with the aim at maximizing the net power output including the consumption of HRU auxiliaries. Table 1 reports the assumptions adopted for the cycle design: among them the most relevant one is the minimum cycle temperature that is selected in order to localize the main compression process close to the critical point of the fluid, exploiting the real gas effects and increasing system efficiency. As additional assumption a reversible mixing process is assumed both at LTR and HTR cold side outlet by varying the split ratio at HRU inlet and HTR inlet respectively. Finally, turbomachinery efficiency and heat exchanger minimum temperature differences have been assumed considering different references from literature although a real industrial benchmark is not available for most components. The optimization variables are the working fluid minimum and maximum pressures and the turbine inlet temperature: for each quantity proper upper and lower bound values are considered in order to obtain a feasible final solution. Heat source is modelled as an ideal gas with a mass flow rate $\dot{m}_{hs}$ of 50 kg/s, a maximum temperature $T_{hs,max}$ of 550°C, a minimum allowable temperature of 150°C and a specific heat capacity $c_{p,hs}$ equal to 1.15 kJ/kg-K, representing a flue gas stream from a combustion process available from either a gas turbine or an industrial process (steel, glass, cement industry).

The numerical model includes also a set of routines for the heat exchangers (HX) design, the calculation of the heat transfer coefficients, the volume of fluid and the mass of the heat exchangers. The recuperators are modelled as printed circuit heat exchangers (PCHE) and main information is derived by the work of Dostal et al. (2004), integrated with manufacturer data and already presented by Alfani et al. (2019). The primary heat exchanger (PHE) is made by two sections: the HTR bypass and the main heater. Both of them are modelled as a finned tube heat exchanger with flue gases flowing outside the tubes. The HRU is modelled as an air-gas cooler equipped with variable rotational speed fans. Performances of HRU is predicted with LU-VE proprietary correlations computing the heat transfer coefficients, the pressure drops and the air flow rate as function of the operating conditions. From the design of each heat exchanger and assuming reasonable piping length between the different components the inventory of $CO_2$ can be calculated. Table 2 reports main assumptions related to the heat exchangers design adopted in this work.

**Table 1**: Heat source data and cycle design assumptions

| **Heat source data and cycle design assumptions** | | | |
|---|---|---|---|
| Heat source mass flow rate $\dot{m}_{hs}$, kg/s | 50 | PHE $CO_2$ $\Delta p$, bar | 2 |
| Heat source temperature $T_{hs,max}$, °C | 550 | HRU $CO_2$ $(\Delta p/p_{in})$ | 0.5% |
| Minimum heat source temperature $T_{hs,min}$, °C | 150 | Recuperators hot side $(\Delta p/p_{in})$ | 0.5% |
| Heat source specific heat $c_{p,hs}$, kJ/kgK | 1.15 | Recuperators cold side $(\Delta p/p_{in})$ | 0.5% |
| Maximum admissible cycle temperature, °C | 525 | Turbine isentropic efficiency, $\eta_{turb}$ | 90% |
| Maximum admissible cycle pressure, bar | 250 | Main compressor efficiency, $\eta_{comp1}$ | 80% |
| Minimum cycle temperature, °C | 33 | Sec. compressor efficiency $\eta_{comp2}$ | 80% |
| LTR pinch point $\Delta T_{LTR}$,°C | 10 | Generator/motor efficiency $\eta_{me,t}/\ \eta_{me,c}$ | 96.4% |
| HTR pinch point $\Delta T_{HLTR}$,°C | 10 | HRU electric consumption per MW of heat rejected $\xi$ | 0.0085 |
| PHE pinch point $\Delta T_{PHE}$,°C | 25 | | |

**Table 2**: Main assumptions for the heat exchangers design

| **Heat exchangers design assumptions** | | | |
|---|---|---|---|
| **PHE and HTR bypass** | | **PCHE** | |
| Tube internal diameter, mm | 20 | Thickness of plate, mm | 1.5 |
| Ratio of tube pitch to external diameter | 1.25 | Diameter of semi-circular channel, mm | 2 |
| Ratio of finned to plain external area | 12 | Thickness of wall between channels, mm | 0.4 |
| Tube material | Carbon steel | Heat exchanger material | INCOLOY800 |

The main indexes used to evaluate the system performance are the cycle net efficiency (including HRU auxiliaries consumption) $\eta_{cycle}$, the heat recovery factor $\chi$ and the overall recovery efficiency $\eta_{rec}$ defined as:

$$\eta_{cycle} = \frac{\dot{W}_{net}}{\dot{Q}_{in,cycle}} = \frac{\dot{W}_t - \dot{W}_{c1} - \dot{W}_{c2} - \dot{W}_{HRU,aux}}{\dot{Q}_{in,cycle}} \qquad \text{Eq.1}$$

$$\chi = \frac{\dot{Q}_{in,cycle}}{\dot{Q}_{hs,max}} = 1 - \frac{\int_{T_{hs,min}}^{T_{stack}} \dot{m}_{hs} cp_{hs}(T) dT}{\int_{T_{hs,min}}^{T_{hs,max}} \dot{m}_{hs} cp_{hs}(T) dT} \qquad \text{Eq.2}$$

$$\eta_{rec} = \chi\, \eta_{cycle} = \frac{\dot{W}_{net}}{\dot{Q}_{hs,max}} \qquad \text{Eq.3}$$

### 2.2 Off-design analysis

The analysis of the system in part load conditions is carried out varying the flue gases mass flow rate between 30-100% of the nominal value. Both heat source maximum temperature and cycle maximum temperature are kept equal to the nominal ones in order to avoid metal over-temperature. Similarly, both ambient air temperature and minimum $CO_2$ temperature are always equal to the nominal values at any part load condition neglecting the effect of seasonality. Each part load solution is obtained by correcting the HX pressure drops, the HX heat transfer coefficients and fan consumption with proper correlations and by verifying energy and mass balances on each component. The heat exchangers areas estimated in design conditions and the off-design overall heat transfer coefficients are used to estimate the temperatures of the streams exiting each heat exchanger and thus to completely define the new operating conditions. Pressure drops ($\Delta$p), heat transfer coefficients (h) and fan consumptions ($\dot{W}_{HRU,aux}$) are calculated with reference to the nominal value and adopting the exponential functions reported in eq.4-6 (Crespi et al. 2017), except for HRU unit that adopts ad hoc correlations. Turbomachinery efficiency variation at part load is for simplicity neglected.

$$\Delta p = \Delta p_{design} \left(\frac{\rho_{design}}{\rho}\right)\left(\frac{\dot{m}}{\dot{m}_{design}}\right)^2 \qquad \text{Eq.4}$$

$$h_X = h_{X,design}\left(\frac{\dot{m}_X}{\dot{m}_{X,design}}\right)^{\alpha} \quad \text{with} \begin{cases} X = CO_2 & \alpha = 0.8 \\ X = gas & \alpha = 0.6 \end{cases} \qquad \text{Eq.5}$$

$$\dot{W}_{HRU,aux} = \dot{W}_{HRU,aux,design}\left(\frac{\dot{m}_{air}}{\dot{m}_{air,design}}\right)^{2.78} \qquad \text{Eq.6}$$

The power output can be maximized at any operating point by acting on the cycle minimum and maximum pressures. The possibility to freely vary both pressures strongly depends on the type and features of the turbomachinery and on the possibility of varying the working fluid inventory by extracting or reinjecting $CO_2$ from an appropriate vessel. As a consequence, marked limitations in the part load operation must be considered if compressors are not provided by IGV and/or variable speed, if the turbine can work only in sliding pressure or if the carbon dioxide inventory cannot be varied.

## 3. RESULTS

### 3.1 Plant design performance

In Figure 2.a-c it is possible to see how the cycle that maximizes the overall recovery efficiency, with a maximum temperature of 347°C, represents the best compromise between the cycle efficiency, that increases with the maximum cycle temperature, and the heat recovery factor that decreases for higher stack temperatures.

Figure 3 depicts the optimal cycle T-s and T-Q diagrams, while the main results are reported in Table 3. Net power output of the optimized cycle is 5.21 $MW_{el}$ with a cycle thermodynamic efficiency of 27.0% and a thermal recovery factor equal to 84.0%, combined to obtain an overall recovery efficiency equal to 22.7%.

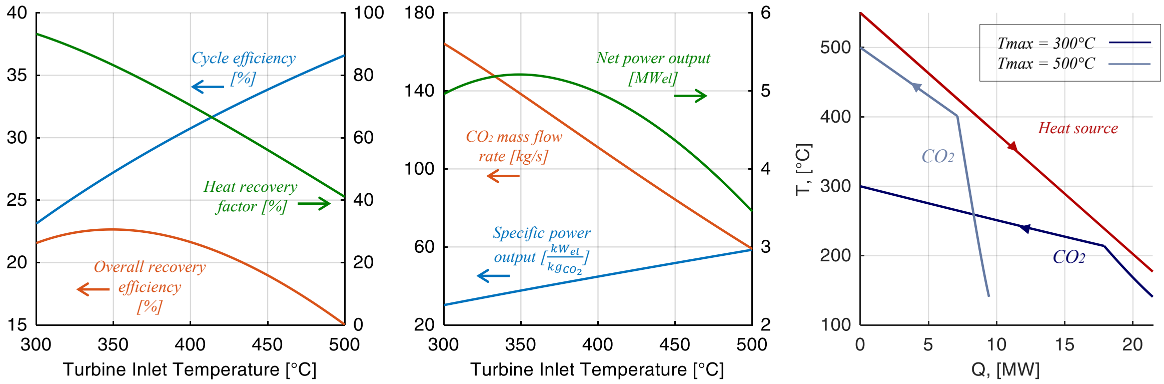


(a) (b) (c)

**Figure 2**: (a) Trends of the main system efficiencies and (b) of the net power output, of the $CO_2$ mass flow rate, of the specific power output as function of the maximum turbine inlet temperature. (c) T-Q diagrams of the sCO2-flue gases heat exchangers for two different cycles maximum temperatures.

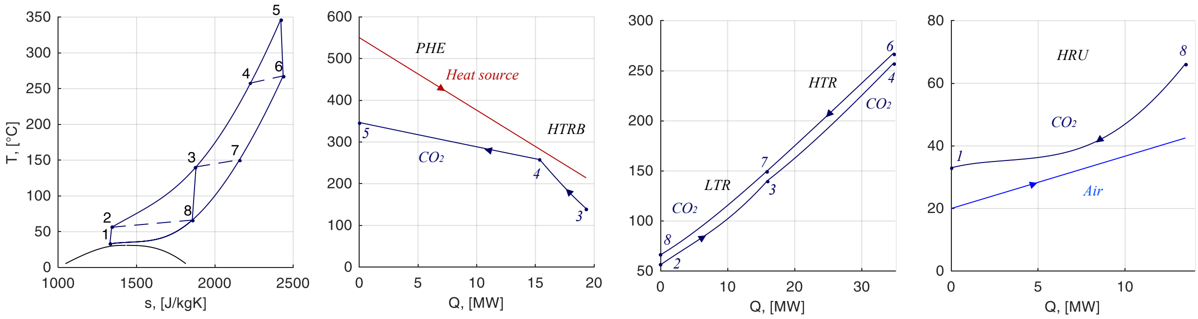


(a) (b) (c) (d)

**Figure 3**: (a) T-s diagram of the best cycle design and corresponding T-Q diagrams of the heat source/$CO_2$ heat exchangers (b), of the cycle recuperators (c) and of the heat rejection unit (d)

**Table 3**: Optimum cycle layout results

| **Cycle design assumptions** | | | |
|---|---|---|---|
| $CO_2$ mass flow at turbine inlet, kg/s | 140.17 | Thermal power recovered, $MW_{th}$ | 19.32 |
| $CO_2$ mass flow at HRU, kg/s | 81.24 | Turbine electric power, $MW_{el}$ | 9.88 |
| $CO_2$ mass flow at HTR bypass, kg/s | 24.37 | Main compressor electric power, $MW_{el}$ | 1.54 |
| Maximum cycle pressure $p_2$, bar | 181.34 | Secondary compressor electric power, $MW_{el}$ | 3.01 |
| Minimum cycle pressure $p_1$, bar | 81.12 | Heat rejection auxiliaries consumption, $kW_{el}$ | 114.46 |
| Turbine inlet temperature $T_5$, °C | 346.69 | **Cycle thermodynamic efficiency** | **26.97%** |
| Heat source outlet temperature, °C | 214.06 | **Heat recovery factor** | **83.99%** |
| Heat source temperature at HTRB inlet, °C | 282.80 | **Overall recovery efficiency** | **22.65%** |

### 3.2 Plant off-design performance

In this section the main results attainable with the presented methodology are reported. A first analysis is carried out varying the heat source mass flow rate in the range 30%-100%, considering a sliding pressure turbine and maintaining a fixed cycle minimum pressure. The trend of specific power production, cycle thermodynamic efficiency, heat recovery factor and overall recovery efficiency will be discussed considering the changes in T-s and T-Q diagrams. A second analysis focuses on the effects of varying the cycle minimum pressure and highlighting the advantages in terms of power output attainable at lower loads and the beneficial effects on compressors operating point. Finally, the last analysis is repeated only for the nominal minimum cycle pressure by keeping the cycle maximum pressure equal to its design value acting on turbine IGV or partial admission arc, showing the potential of a fine control of all the turbomachinery in terms of plant reliability and power output. Fluid inventory trend for all the different part load strategies is reported and discussed.

*3.2.1 CASE1: Sliding pressure turbine and fixed minimum pressure*

Figure 4.a depicts the trend of specific power output calculated as the ratio between the net power output and the heat source mass flow rate. This quantity remains stable until 60% of the thermal input

while it drops for lower loads loosing around 30% of the nominal efficiency. This loss of efficiency can be motivated by considering the trend of thermodynamic cycle efficiency and heat recovery factor (Figure 4.c). For heat source mass flow rate values ranging from the nominal value to 60%, the lower cycle pressure ratio is compensated by the lower temperature differences and the higher effectiveness of the recuperators and of the PHE, so that the stack temperature remains relatively stable as shown by corresponding T-s and TQ diagrams for the cycle at 60% of the load (Figure 4.b and Figure 4.e). Moreover, the increase of $CO_2$ temperature at PHE inlet (point 4 in Figure 3.a) due to the reduction of the pressure ratio is balanced by the decrease of the temperature at the exit of the LTR (point 3 in Figure 3.a).

For lower loads instead the cycle efficiency is penalized by the excessive reduction in the pressure ratio of the cycle, which limits the turbine specific work and the net output of the cycle. Furthermore, the strong reduction of the $CO_2$ mass flow rate penalizes the HX heat transfer coefficients limiting the internal heat regeneration of the cycle.

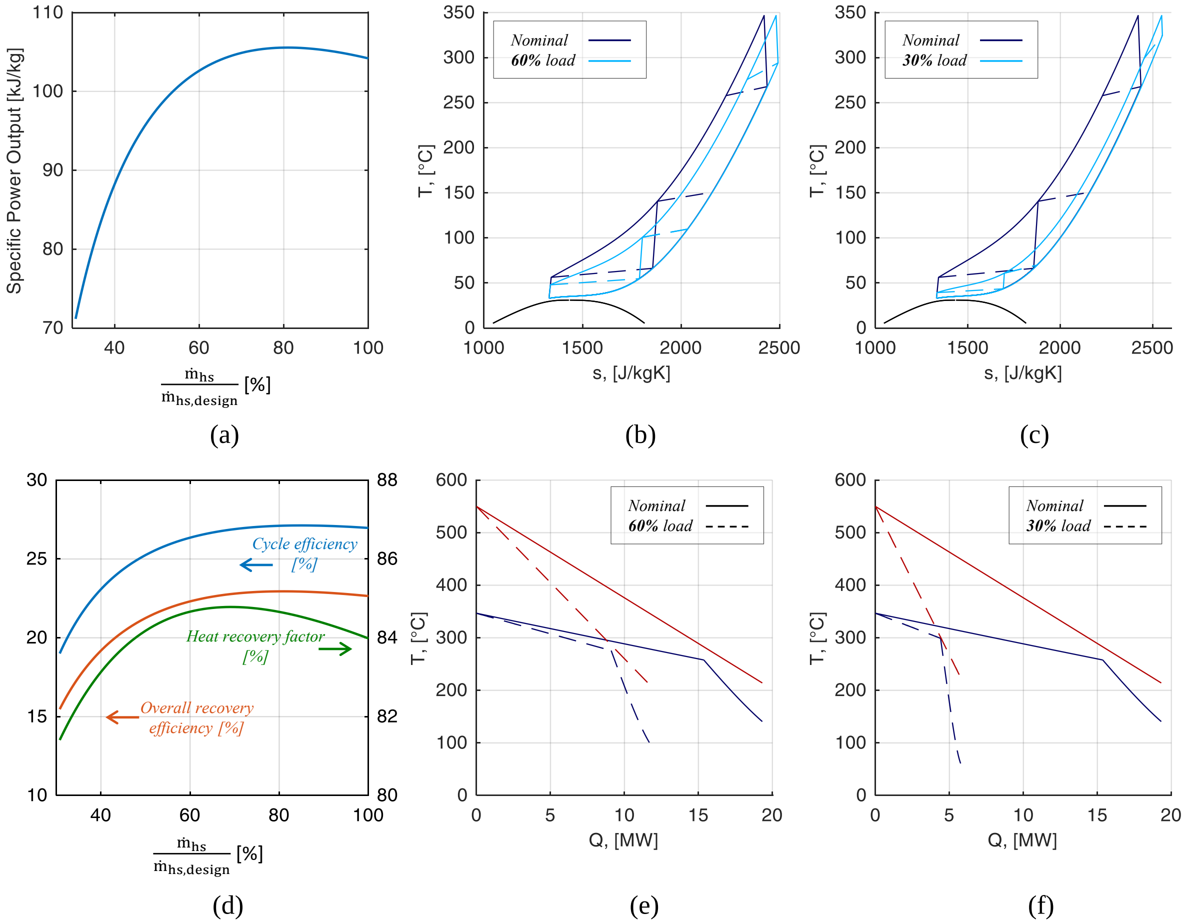


**Figure 4**: (a) Specific power output as function of the heat source mass flow rate, (b) design T-s diagram vs T-s diagrams at 60% and (c) 30% of the heat source mass flow rate, (d) main efficiencies as function of the heat source mass flow rate, (e) design T-Q diagram vs T-Q diagram at 60% and (f) 30% of the heat source mass flow rate

*3.2.2 CASE2: Sliding pressure turbine and optimization of the minimum cycle pressure*

As highlighted by the previous analysis at lower loads would be positive to increase the cycle pressure ratio in order to limit the penalization on cycle efficiency and heat recovery efficiency. A sensitivity analysis is carried out for six different minimum cycle pressures down to 0.95 of the nominal one. Figure 5.a depicts the trend of specific power output and it is possible to note that optimal minimum pressure decreases for lower mass flows of flue gases and in particular a value equal to 0.95 the nominal is the optimal solution at minimum heat source mass flow rate. Acting on the cycle minimum pressure allows in this case increasing the net power output by approximately 8%.

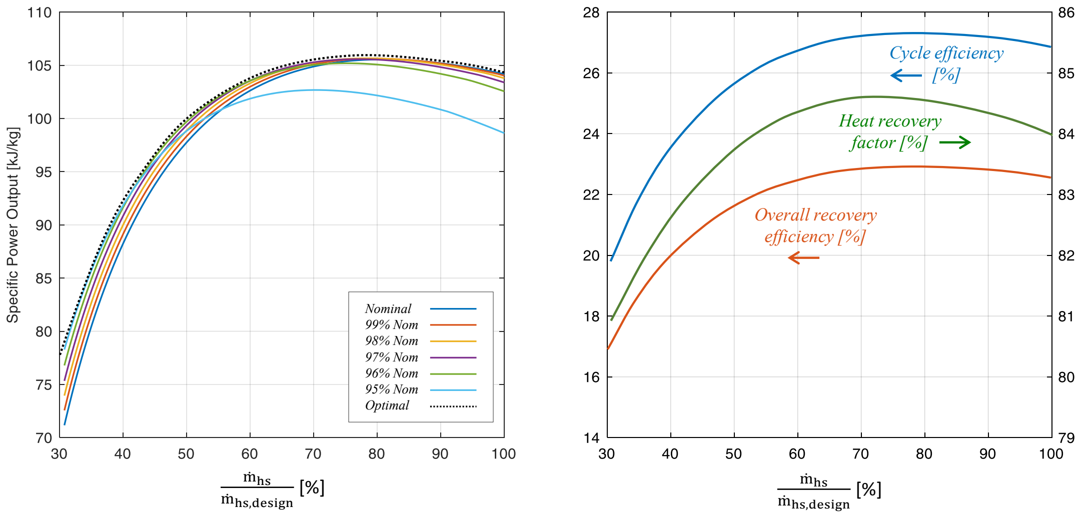


(a) (b)

**Figure 5**: (a) cycle specific power output for different cycle minimum pressures and (b) main efficiencies as function of the heat source mass flow rate for the optimal minimum pressure (CASE2)

Moreover, it is interesting to note how the operating points of the main and the secondary compressor change depending on the strategy adopted for the control of cycle minimum pressure. Figure 6.b and Figure 6.c show the operative range of the two compressors in terms of enthalpy head and volume flow rate with respect to the nominal case for the fixed and for the optimized minimum pressure cases. These limits are just qualitative as they have been obtained through a preliminary design performed within the $sCO_2$-Flex project for compressors equipped both with IGV and variable speed (60%;105%) for a different application, a coal-fired power plant. Line on the top-left represents the surge limit, while line on the bottom-right represents the choke limit. Info on compressor efficiency are protected by NDA but it can be stated that compressor performance remains pretty close to the nominal while moving on an operative line parallel to the surge limit while it strongly decreases working close to the choke line. With fixed minimum pressure (CASE1) at minimum load both main and secondary compressors working point fall within the operative region, except for very low mass flow rate of flue gases (<35%).

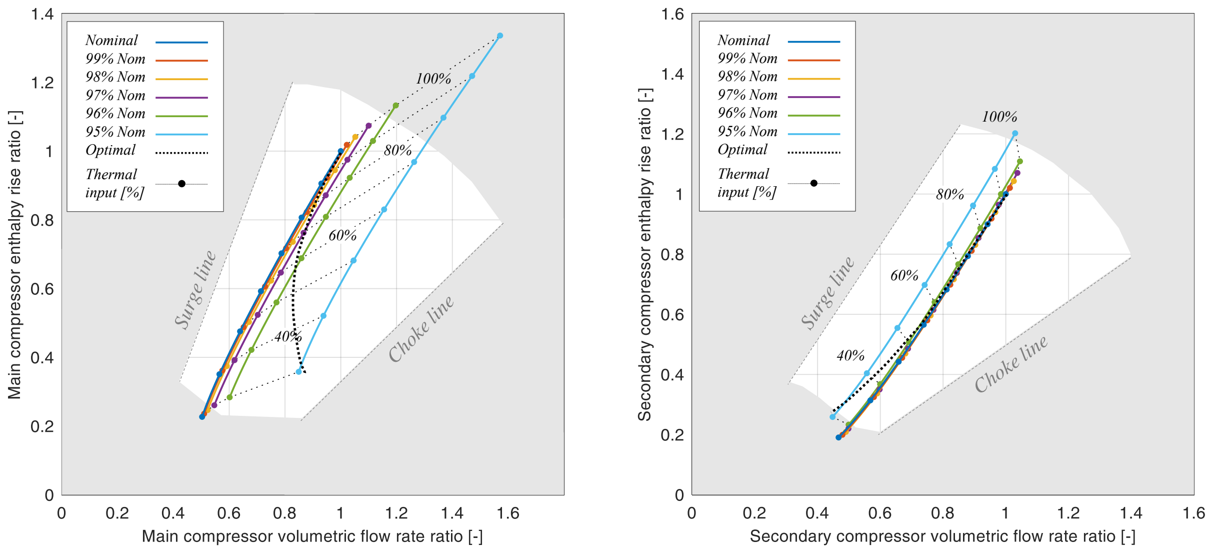


(a) (b)

**Figure 6**: (a) Main and (b) secondary compressor operating points for the fixed minimum cycle pressure equal to the nominal value (CASE 1) and for variable minimum pressure case (CASE 2) as function of the fuel input. The white area in the figure represents the operating region for the main compressor with VIGV and variable rotating speed.

Decreasing the minimum pressure of the cycle in order to maximize the overall efficiency (CASE2) increases the volume flow rate and the enthalpy head in the primary compressor, allowing operation down to 30% of the nominal mass flow rate flue gases. However, the operative points move towards the low efficiency region involving a possible penalization of the system efficiency that should be carefully evaluated. By varying the minimum pressure also the secondary compressor can manage lower loads, in this case with a reduced volumetric flow rate. One further degree of freedom not investigated in this work is related to the possibility of varying the split ratio (SR) and thus act both on the main and secondary compressor volumetric flows or increasing the cycle minimum temperature by reducing HRU fan speed. It is important to underline once again that a more detailed investigation considering also the variation of turbomachinery isentropic efficiency is necessary to evaluate the best operating strategy at part load.

*3.2.3 CASE3: Advantages related to turbine control in part load*

A further possibility in order to increase part load performance of $sCO_2$ power plants is to provide the turbine with IGV or partial admission arc in order to control the cycle maximum pressure instead of allowing its variation in sliding pressure. Both features can be adopted on this turbomachine because of the low fluid maximum temperature and the choice depends mainly on the size and the type of the component (radial centripetal vs axial turbine). With this control strategy the cycle efficiency and the overall recovery efficiency at part load increase with respect to the nominal value, thanks to the increased heat exchanger effectiveness and thanks to the quasi-constant cycle compression ratio. The overall recovery efficiency trend with respect to the sliding pressure cases is reported in Figure 7.a.
A severe drawback of this control strategy, however, is related to the main and secondary compressors operating points (see Figure 7.b and c): already at 80% of the heat source flow rate the operating point of the main compressors moves towards the surge zone, crossing it for a value around 72% and 68% of the flue gas mass flow rate for the primary and secondary compressor respectively. This fact not only limits significantly the initial hypothesis on constant turbomachinery efficiency since compressor recirculation bypass is activated. A possible solution to overcome this problem is the adoption of different compressors in parallel that can be switched off as the load is reduced; it is important to underline anyhow that smaller compressors may be characterized by lower performance and higher total investment cost. Other solutions may imply the selection of a different compressor design point, the variation of the minimum cycle pressure as for the sliding pressure case in order to positively influence the volumetric flow at the compressor inlet or the variation of the split ratios at the HRU inlet and at the HTR.

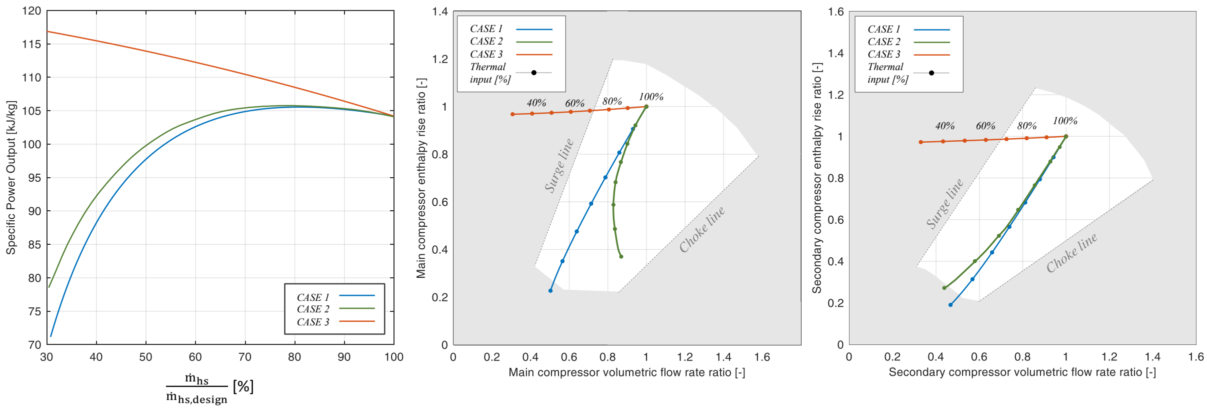


(a) (b) (c)

**Figure 7**: (a) variation of plant efficiency with the flue gases mass flow rate for the three different investigated part load strategies and (b) main and (c) compressor operating points for CASE 1, CASE 2 and CASE 3 as function of the fuel input. The white area in the figure represents the operating region for the main compressor with VIGV and variable rotating speed.

### 3.3 Effect on working fluid inventory

A last discussion shall concern the variation of working fluid inventory that represents a specific aspect of closed gas cycles. The lack of hot wells in the systems (where variation of fluid volume can be accommodated in liquid state) involves that the cycle operating conditions directly determine the mass of fluid within the cycle. The part load control of closed ideal gas cycles can be obtained by cycle de-pressurization, meaning removing a fraction of the fluid mass in order to reduce the cycle pressure levels and allowing the turbomachinery to work close to nominal conditions. For $sCO_2$ cycles the same strategy can be applied although it is complicated by the presence of strong real gas effects close to the critical point that determines large variations of fluid compressibility factor for small changes of operating conditions. Moreover, it is important to underline that the inventory variation needs additional components and additional control systems that may increase the cost of the system and limit the flexibility. Figure 8 depicts the inventory variation with respect to the nominal for all the different presented strategies: for the sliding pressure cases the working fluid inventory within the plant decreases, meaning that at part load a fraction of $CO_2$ must be removed from the system and stored in a vessel. If the maximum pressure is kept constant on the other hand, the inventory variation is just slightly decreasing at partial load, with potential advantages in terms of dynamic control of the system and in terms of investment costs.

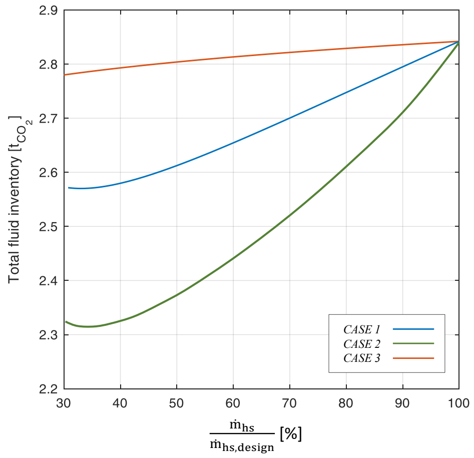


**Figure 8**: Variation of $CO_2$ inventory for the three different investigated strategies

## 4. CONCLUSIONS

In the present work, the study of a recuperative recompressed $sCO_2$ cycle with HTR bypass as power cycle for waste heat recovery from a hot gas stream at 550°C was performed. A maximum overall recovery efficiency of 22.65% was obtained for a maximum cycle temperature and pressure of 346.7°C and 181.3 bar respectively and for a minimum pressure of 81.1 bar. Once a preliminary design of all the main heat exchangers was performed, different part load operating strategies were compared in order to identify their impact on the plant efficiency and on the operating points of the main and secondary compressor. From the overall recovery efficiency point of view keeping the same turbine inlet pressure at part load guarantees the best performance with an increase of plant efficiency at part load thanks to the increased recuperators efficiency. This operating strategy guarantees also a negligible $CO_2$ inventory variation, but on the other hand cannot be pursued with a single main compressor but requires more compressors in parallel or the use of recirculation bypass with a consequent penalization of system efficiency. If the turbine works in sliding pressure and minimum cycle pressure is constant the plant efficiency slightly increases at 75% load but then it is strongly penalized for lower loads. The optimization of the minimum cycle pressure has marked impact on the plant efficiency (about 11% more at minimum load) but the advantage should be carefully evaluated taking into account also the variation of the compressors and turbine isentropic efficiencies. For both those strategies the $CO_2$ inventory changes significantly. Future development of this work will include the study of the impact of the turbomachinery efficiency variation with the operating conditions and will investigate further operational degrees of freedom such as variation of the split ratios or a combination of different control strategies.

## NOMENCLATURE

***Symbols***

| | |
|---|---|
| A | Area ($m^2$) |
| cp | Specific Heat Capacity (J/kgK) |
| h | Heat Transfer Coefficient ($W/m^2$-K) |
| $\dot{m}$ | Mass Flow Rate (kg/s) |
| $\dot{Q}$ | Thermal Power (W) |
| T | Temperature (°C) |
| U | Overall heat transfer coefficient ($W/m^2$-K) |
| $\dot{W}$ | Power (W) |
| $\eta$ | Efficiency (%) |
| $\xi$ | Specific HRU Elec. Cons. ($W_{el}$/ $W_{th}$) |

***Acronyms***

| | |
|---|---|
| APH | Air Preheater |
| HRU | Heat Rejection Unit |
| LTR | Low Temperature Recuperator |
| HTR | High Temperature Recuperator |
| HTRB | High Temperature Rec. Bypass |
| HX | Heat Exchanger |
| PCHE | Printed Circuit Heat Exchanger |
| PHE | Primary Heat Exchanger |
| $SCO_2$ | Supercritical $CO_2$ |
| SR | Split Ratio |
| VIGV | Variable Inlet Guide Vane |

## AKNOWLEDGEMENTS

The sCO2-Flex project has received funding from the European Union's Horizon 2020 research and innovation programme under grant agreement N° 764690.

## REFERENCES

Alfani, Dario, Marco Astolfi, Marco Binotti, Stefano Campanari, Francesco Casella, and Paolo Silva. 2019. "Multi Objective Optimization of Flexible Supercritical CO2 Coal-Fired Power Plant." In *ASME Turbo Expo 2019: Turbomachinery Technical Conference and Exibition*. Phoenix, Arizona, USA.

Astolfi, Marco, Dario Alfani, Silvia Lasala, and Ennio Macchi. 2018. "Comparison between ORC and CO2 Power Systems for the Exploitation of Low-Medium Temperature Heat Sources." *Energy* 161 (October): 1250–61. https://doi.org/10.1016/J.ENERGY.2018.07.099.

Binotti, Marco, Marco Astolfi, Stefano Campanari, Giampaolo Manzolini, and Paolo Silva. 2017. "Preliminary Assessment of SCO2cycles for Power Generation in CSP Solar Tower Plants." *Applied Energy* 204 (October): 1007–17. https://doi.org/10.1016/j.apenergy.2017.05.121.

Crespi, Francesco, Giacomo Gavagnin, David Sánchez, and Gonzalo S. Martínez. 2017. "Supercritical Carbon Dioxide Cycles for Power Generation: A Review." *Applied Energy* 195: 152–83. https://doi.org/10.1016/j.apenergy.2017.02.048.

Crespi, Francesco, David Sánchez, Kevin Hoopes, Brian Choi, and Nicole Kuek. 2017. "The Conductance Ratio Method for Off-Design Heat Exchanger Modeling and Its Impact on an SCO2 Recompression Cycle." In *ASME Turbo Expo 2017: Turbomachinery Technical Conference and Exposition GT2017*, V009T38A025. https://doi.org/10.1115/gt2017-64908.

Dostal, V, M J Driscoll, and P Hejzlar. 2004. "Advanced Nuclear Power Technology Program A Supercritical Carbon Dioxide Cycle for Next Generation Nuclear Reactors."

Ho, Clifford K., Matthew Carlson, Pardeep Garg, and Pramod Kumar. 2016. "Technoeconomic Analysis of Alternative Solarized S-CO $_2$ Brayton Cycle Configurations." *Journal of Solar Energy Engineering* 138 (5): 051004. https://doi.org/10.1115/1.4033573.

Lemmon, E.W., M.L. Huber, and M.O. McLinden. 2013. "NIST Standard Reference Database 23: Reference Fluid Thermodynamic and Transport Properties-REFPROP, Version 9.1,." Gaithersburg: National Institute of Standards and Technology.

"LU-VE S.p.A. - Heat Exchangers for Refrigeration and Air Conditioning." n.d.

Macchi, Ennio., and Marco. Astolfi. 2016. *Organic Rankine Cycle (ORC) Power Systems.* Elsevier Science.

Mecheri, Mounir, and Yann Le Moullec. 2016. "Supercritical CO2 Brayton Cycles for Coal-Fired Power Plants." *Energy* 103: 758–71. https://doi.org/10.1016/j.energy.2016.02.111.

Polimeni, S., M. Binotti, L. Moretti, and G. Manzolini. 2018. "Comparison of Sodium and KCl-MgCl2 as Heat Transfer Fluids in CSP Solar Tower with SCO2 Power Cycles." *Solar Energy* 162. https://doi.org/10.1016/j.solener.2018.01.046.